Journal of Zhejiang University SCIENCE B
ISSN 1673-1581 (Print); ISSN 1862-1783 (Online)
www.zju.edu.cn/jzus; www.springerlink.com
E-mail: jzus@zju.edu.cn

Hydraulic pressure inducing renal tubular epithelial-myofibroblast transdifferentiation in vitro*

Fei-yan LI[§1], Xi-sheng XIE[§1], Jun-ming FAN[†‡1,2], Zi LI[1], Jiang WU[3], Rong ZHENG[1]

([1]*Department of Nephrology, West China Hospital of Sichuan University, Chengdu 610041, China*)

([2]*State Key Laboratory of Biotherapy of Human Disease, West China Hospital of Sichuan University, Chengdu 610041, China*)

([3]*Institute of Biomedical Engineering, West China Center of Medical Sciences, Sichuan University, Chengdu 610041, China*)

[†]E-mail: junmingfan2007@yahoo.com.cn

Received Apr. 18, 2009; Revision accepted June 19, 2009; Crosschecked July 28, 2009

Abstract: Objective: The effects of hydraulic pressure on renal tubular epithelial-myofibroblast transdifferentiation (TEMT) were investigated. Methods: We applied hydraulic pressure (50 cmH_2O) to normal rat kidney tubular epithelial cells (NRK52E) for different durations. Furthermore, different pressure magnitudes were applied to cells. The morphology, cytoskeleton, and expression of myofibroblastic marker protein and transforming growth factor-β1 (TGF-β1) of NRK52E cells were examined. Results: Disorganized actin filaments and formation of curling clusters in actin were seen in the cytoplasm of pressurized cells. We verified that de novo expression of α-smooth muscle actin induced by pressure, which indicated TEMT, was dependent on both the magnitude and duration of pressure. TGF-β1 expression was significantly upregulated under certain conditions, which implies that the induction of TEMT by hydraulic pressure is related with TGF-β1. Conclusion: We illustrate for the first time that hydraulic pressure can induce TEMT in a pressure magnitude- and duration-dependent manner, and that this TEMT is accompanied by TGF-β1 secretion.

Key words: Hydraulic pressure, Tubular epithelial-myofibroblast transdifferentiation, Transforming growth factor-β1 (TGF-β1)
doi:10.1631/jzus.B0920110 **Document code:** A **CLC number:** Q813; R68

INTRODUCTION

Human beings experience diverse mechanical forces from a wide variety of sources. Certain mechanical forces play a normal, fundamental role in the regulation of cell functions, including gene induction, protein synthesis, and cell growth, death, and differentiation. However, abnormal mechanical forces alter cellular function and change the structure and composition of the extracellular matrix, eventually leading to tissue or organ pathologies, as well as fibrosis (Wang and Thampatty, 2006). For example, some studies have shown that pressure can influence the morphology, skeleton, proliferation, apoptosis, and secretion function of endothelial cells (Lehoux *et al*., 2006; Shin *et al*., 2002; Silverman *et al*., 1999).

Indeed, mechanical forces are involved in kidney diseases and changes in cellular function. In diabetic kidney disease, mechanical forces may aggravate a metabolic insult by stimulating excessive cellular glucose uptake, which, in turn, causes damage to the kidney (Gnudi *et al*., 2007). Pressure can induce expression of monocyte chemoattractant protein in mesangial cells (Suda *et al*., 2001). One model of hypertension suggests that pressure can lead to renal interstitial fibrosis, tubular necrosis, and interlobular artery injury (Mori and Cowley, 2004). Since the early 1980s, the "hyperfiltration theory" has been of great interest in nephrology and hypertension. This theory predicts that, when a renal mass is reduced, which is observed in a large number of renal diseases (Klahr *et al*., 1988), adaptations in the microcirculation of remnant

‡ Corresponding author
§ The two authors contributed equally to this work
* Project (No. 2007CB947802) supported by National Basic Research Program of China

glomeruli increase the mean driving force for filtration and therefore markedly increase the glomerular capillary pressure in remnant glomeruli (Deen *et al*., 1974; Kaufman *et al*., 1975).

Renal mass reduction is followed rapidly by a dramatic increase in glomerular filtration rate in the remaining nephrons. Micropuncture studies have shown a threefold increase in glomerular filtration rate in the remaining nephrons soon after partial nephrectomy and a significant increase in the proximal tubular pressure (Hostetter *et al*., 1981). The apical pole of renal tubular cells is bathed by the tubular fluid. The flow rate is fairly stable in this tube under normal physiological conditions, but when there is a substantial reduction in renal mass, it may increase dramatically, mainly in the proximal tubule. Studies conducted in vitro using a laminar flow chamber and studies in vivo confirm that tubular flow has pleiotropic effects on proximal tubular cells (Essig *et al*., 2001) and may be one of the causes for tubular damage occurring after renal mass reduction (Essig and Friedlander, 2003).

After renal mass reduction, the hyperfiltration in remnant glomeruli is followed by a progressive destruction of remaining functional nephrons even after the apparent resolution of the initial injury. This deterioration of renal structures was observed in a large number of renal diseases (Klahr *et al*., 1988) and involved renal fibrosis (Rodriguez-Pena *et al*., 2001). Renal fibrosis is the hallmark of chronic kidney disease of diverse causes (Meguid El Nahas and Bello, 2005). Renal tubular epithelial-myofibroblast transdifferentiation (TEMT) involves the loss of epithelial adhesion molecules, de novo expression of α-smooth muscle actin (α-SMA), and actin reorganization, and plays a key role in the progress of renal fibrosis. TEMT is regulated by numerous growth factors, cytokines, and hormones. Transforming growth factor-β1 (TGF-β1) is the most important profibrotic factor in the kidney (Zavadil and Bottinger, 2005). It is possible that changes in mechanical forces also contribute to renal fibrosis. In fact, certain mechanical force has been shown to cause TEMT (Sato *et al*., 2003), which can lead to fibrosis. However, this previous study looked only at stretching force, so whether hydraulic pressure, one of the mechanical forces acting on tubules, can induce renal TEMT remains unknown.

Therefore in this study we examined whether tubular hydraulic pressure contributes to renal fibrosis by inducing TEMT in proximal tubular cells. To our knowledge, this is the first investigation of the effects of hydraulic pressure on TEMT, and it may provide insight into mechanisms of renal TEMT and renal fibrosis.

MATERIALS AND METHODS

Epithelial cell culture

A well-characterized normal rat kidney epithelial cell line (NRK52E) was obtained from the American Type Culture Collection (Rockville, MD, USA). NRK52E cells were seeded into culture flasks (Corning, Japan) and cultured at 37 °C in a 5% CO_2 environment. The culture medium consisted of Dulbecco's modified Eagle's medium (DMEM, Hyclone, USA) supplemented with 10% (w/v) fetal bovine serum (Hyclone, USA) and penicillin-streptomycin (Hyclone, USA). Cells were seeded onto glass slides for 24 h and then placed in a flow chamber for pressure loading.

Hydraulic pressure-loading experiments

Our assembly consisted of a damping chamber, a flow chamber, a reservoir, and a roller pump (Millipore, USA). The flow chamber was composed of the cell culture chamber, an I/O unit, and a silicone gasket. The height of the reservoir controlled the force of the hydraulic pressure applied to the NRK52E cells in the flow chamber. Medium was equilibrated with 5% CO_2/95% air, and the temperature was maintained at 37 °C. A similar assembly of the hydraulic pressure apparatus has been used in previous studies (Cheng *et al*., 2007; Ohashi *et al*., 2007).

We performed two experiments in our study. During the first pressure-loading experiment, cells were exposed to a hydraulic pressure of 50 cmH_2O for 2, 6, 12, and 24 h to investigate whether the TEMT depended on the duration of pressure applied. In the second experiment, we applied pressures of different magnitudes (30, 50, or 100 cmH_2O) for 24 h to examine the correlation of pressure magnitude with TEMT. Because static pressure does not mimic physiological environments of renal tubule, we carried out our experiments in a flow chamber to mimic

the in vivo environment. Since a previous study showed that shear stress of 0.1~0.5 Pa in vivo can affect NRK52E cells (Cowger *et al*., 2002), we applied a shear stress of 0.1 Pa to cells to avoid the influence of abnormal shear stress. In all experiments, we included two control groups to check for effects of shear stress: a normal control group, in which cells were cultured for 24 h in a normal incubator, and a shear stress control group, in which cells were cultured in the flow chamber but without applied hydraulic pressure for 24 h.

All the cells in each group were collected for isolation of total protein and RNA. The supernatants were preserved at –20 °C for enzyme-linked immunosorbent assay (ELISA). Cells of the first experiment were fixed with immunocytochemistry staining for electron microscopy.

Immunocytochemistry

Confluent cells were fixed in 10% (w/v) formaldehyde for 30 min and permeabilized in 0.1% (v/v) Triton X-100 for 10 min. Then cells were incubated with 0.3% (v/v) H_2O_2 for 20 min to inactivate endogenous peroxidases and then with 1:20 (v/v) normal sheep serum for 30 min at 37 °C to block nonspecific binding. After that, cells were first incubated with anti-α-SMA antibody (1:200, Santa Cruz, USA) for 2 h at 37 °C, then with goat anti-mouse horseradish peroxidase (HRP)-immunoglobulin (IgG) (1:200, Santa Cruz, USA) for 1 h at 37 °C. The cells were then stained with diaminobenzidine (DAB). In this way, the primary antibody was stained by sequential incubations to produce a brown color. Finally, cells were stained with hematoxylin, dehydrated through graded ethanol (80%, 95%, and 100%, v/v), cleared with dimethylbenzene, and coverslipped using an aqueous mounting medium.

Scanning electron microscopy

Both pressurized and nonpressurized cells were fixed in 2.5% (v/v) glutaraldehyde in phosphate-buffered saline (PBS) for 60 min, rinsed with PBS, and dehydrated through graded ethanol (30%, 50%, 70%, 80%, 90%, 95%, and 100% (v/v) for 10 min each). Cells were then transferred to amyl acetate for 10 min, put on critical point drying, and then coated with gold. Cells were viewed through a scanning electron microscope (Olympus, Japan).

F-actin filaments staining

Cells were fixed with 10% (w/v) formaldehyde for 30 min and permeabilized with 0.1% (v/v) Triton X-100 for 10 min to allow F-actin staining. F-actin filaments were then stained with fluorescein isothiocyanate (FITC)-conjugated phalloidin (Sigma, USA). Fluorescence images were observed using a fluorescence microscope (Nikon, Japan). The percentage of cells with F-actin filaments or F-actin cluster was calculated. Status of F-actin was quantitated by random choosing 20 microscopic fields and counting cells in the field as either with F-actin filaments or F-actin cluster.

Western blotting analysis

Western blotting analysis was used to measure the levels of α-SMA protein in pressurized and control cells. Cell lysates were prepared by scraping cells from the dish with a cell scraper into 100 μl of cell protein extraction reagent (Kangchen Co., China) containing inhibitor cocktails against proteases and phosphatases (Kangchen Co., China). Total protein concentration was measured by the Bradford protein assay kit (GALEN, China). Lysates (20 μl) were separated by sodium dodecyl sulfate (SDS)-polyacrylamide gel electrophoresis and transferred to polyvinylidene difluoride (PVDF) membrane (Millipore, USA). Non-specific background was blocked by washing with 5% (w/v) non-fat dried milk in Tris buffered saline Tween-20 (TBST) for 1 h. The membrane was then incubated overnight with primary antibody against α-SMA (Santa Cruz, USA). After that, membranes were incubated with HRP-conjugated secondary antibody for 1 h at room temperature. Then antibody binding was detected using the electrochemiluminescence (ECL) detection kit to produce a chemiluminescence signal, which was captured on X-ray film. Band intensity was quantified from scanned membrane images using the National Institutes of Health (NIH) Image software. To ensure that the results obtained by Western blotting were not due to unequal protein loading or transfer, Western blotting against β-actin was routinely carried out in parallel.

Real-time polymerase chain reaction (PCR)

To measure the mRNA levels of α-SMA and TGF-β1, total RNA was extracted from cells by the Trizol method (Sigma, USA). The cDNA was

synthesized using 500 ng of total RNA with the PrimeScript™ reverse transcription-polymerase chain reaction (RT-PCR) kit (Takara, Japan). Real-time RT-PCR was performed using the SYBR Green real-time PCR Master Mix (Toyobo, Japan). Primers of α-SMA, TGF-β1, and the internal control glyceraldehyde-3-phosphate dehydrogenase (GAPDH) were synthesized by Invitrogen (Shanghai, China) (Table 1). PCR reactions (20 μl) contained the following: 10 μl of SYBR Green real-time PCR Master Mix, 0.5 μl of forward primer, 0.5 μl of reverse primer, 1 μl of cDNA, and 8 μl of diethypyrocarbonate (DEPC)-H_2O. Reactions were amplified in a Roche LightCycler (Roche, USA) under the following conditions: initial denaturation at 94 °C for 1 min, 50 cycles of denaturation at 94 °C for 10 s, annealing at 59 °C for 10 s, and polymerization at 72 °C for 10 s. PCR products were analyzed by agarose electrophoresis. In the real-time PCR process, the fluorescence signal was collected during the polymerization steps. In order to examine the efficiency of real-time PCR, standard curves were established using serial dilutions of sample cDNA. The standard curves were used to measure the gene expression levels of the target gene and the reference GAPDH gene using Roche LightCycler software 4.05. Expression of the target gene was normalized to GAPDH expression.

Table 1 Nucleotide sequences of primers

Gene	Primer sequences
α-SMA	Forward: 5′-atccgatagaacacggcatc-3′ Reverse: 5′-agtcacgccatctccagagt-3′
TGF-β1	Forward: 5′-tacagggctttcgcttcagt-3′ Reverse: 5′-gtccaggctccaaatgtagg-3′
GAPDH	Forward: 5′-gcaagttcaacggcagca-3′ Reverse: 5′-cgccagtagactccacgac-3′

Enzyme-linked immunosorbent assay (ELISA)

TGF-β1 concentrations in the supernatants of NRK52E cells were measured using an ELISA kit (R&D, USA) following the method recommended by the manufacturer. The supernatants of pressure-loaded cells were concentrated to 5 ml by lyophilization. The concentrated samples, together with standards containing known amounts of rat TGF-β1, were added to flat-bottomed 96-well ELISA plates coated with monoclonal antibody specific for rat TGF-β1 and incubated at 37 °C for 2 h. Then the biotinylated monoclonal antibody specific for rat TGF-β1 was added and incubated at 37 °C for 1 h. After removal of excess second antibody, streptavidin-peroxidase was added and incubated at 37 °C for 1 h. Then, a substrate solution was added to interact with the bound enzyme in order to produce color. The intensity of this colored product was directly proportional to the concentration of TGF-β1 present in the sample. The absorbance at 492 nm was analyzed and used to calculate the concentration of TGF-β1 in the sample based on a standard curve.

Statistical analysis

Inter-group statistical comparisons were made by a one-way analysis of variance (ANOVA) using SPSS 13.0 software. A value of $P<0.05$ was considered significant in ANOVA analyses.

RESULTS

Morphology of NRK52E cells under hydraulic pressure

Normal cultured NRK52E cells exhibited the epithelial cobblestone morphology under inverted phase contrast microscopy. Scanning electron microscopy shows that these cells had a cubic or round shape and many microvilli on the cell surface (Fig.1a). Morphology of shear stress control cells under light or electron microscopy was the same as that of normal cells. All the pressurized cells retained the epithelial cobblestone morphology similar to the normal control cells under inverted phase contrast microscopy. However, by scanning electron microscopy, the cells exposed to hydraulic pressure of 50 cmH_2O for 12 or 24 h showed a slightly spindle-like shape, elongation and loss of cell junction and microvilli on the cell surface (Fig.1b).

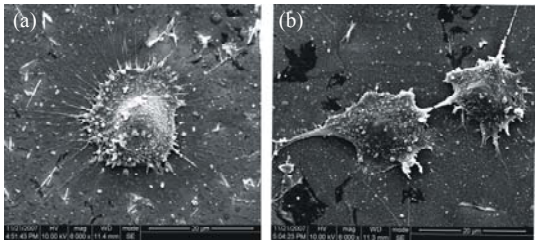

Fig.1 NRK52E cells under the scanning electron microscopy. (a) Normal cultured NRK52E cells showed a round shape and had many microvilli on the cell surface; (b) Cells held under 50 cmH_2O of pressure for 24 h showed a mildly spindle-like shape and loss of cell junctions and microvilli

Cytoskeletal changes of NRK52E cells under hydraulic pressure

Typical fluorescence images of FITC-phalloidin-stained NRK52E cells are shown in Fig.2. F-actin filaments in normal cells were straight, thin, and cable-like, and they were symmetrically aligned in the cytoplasm and cell membrane. Hydraulic pressure induced disorganization of the F-actin filaments and the formation of curling clusters of F-actin in the cytoplasm. The longer the duration of the pressure-loading was, the smaller the amount of cable-like F-actin filaments (Fig.3a). Furthermore, the number of cells with curling F-actin clusters increased with increasing duration of pressure loading (Fig.3b). It should be noted that in the shear stress control group, a significant amount of cable-like F-actin was observed in the cytoplasm and cell membrane, and these results were similar to those in the normal control group.

Phenotypic changes of NRK52E cells under hydraulic pressure

Since α-SMA is the typical marker of myofibroblasts, mRNA and protein levels of α-SMA were detected. Immunocytochemistry staining is shown in Fig.4. Normal control cells exhibited a normal

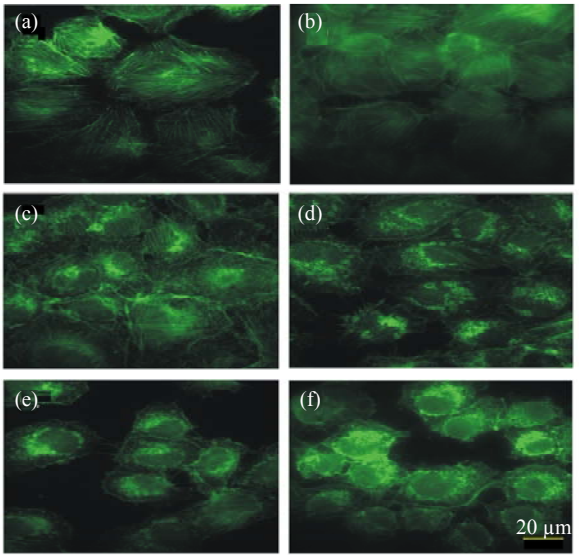

Fig.2 Fluorescence images of NRK52E cells stained with FITC-phalloidin. F-actin filaments in normal cells were straight, thin and cable-like. Hydraulic pressure induced formation of curling clusters of F-actin. The status of F-actin in shear stress control group was similar to that of normal. Normal control cells (a), shear stress control cells (b), and cells held under pressure of 50 cmH_2O for 2 h (c), 6 h (d), 12 h (e), and 24 h (f)

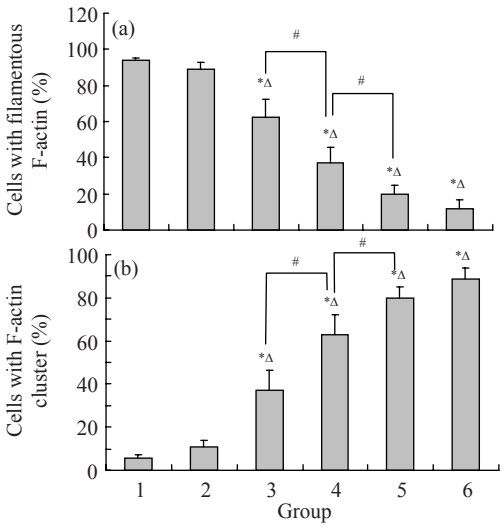

Fig.3 (a) Percentage of cells with filamentous F-actin in the six groups (normal control cells (group 1), shear stress control cells (group 2), and cells held under pressure of 50 cmH_2O for 2 h (group 3), 6 h (group 4), 12 h (group 5), and 24 h (group 6)). The longer the duration of the pressure-loading was, the smaller the amount of cable-like F-actin filaments; (b) Percentage of cells with F-actin cluster in the above six group. The number of cells with F-actin clusters increased with increasing duration of pressure-loading. $^{*}P<0.05$ compared with the normal control group. $^{\Delta}P<0.05$ compared with the shear stress control group. $^{\#}P<0.05$ ($n=6$)

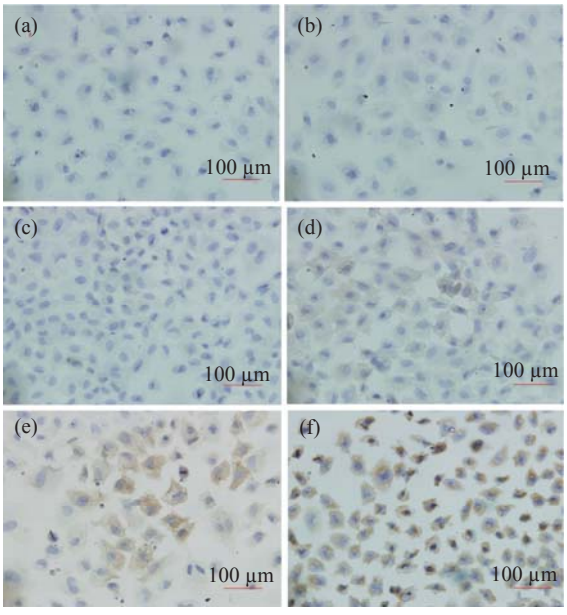

Fig.4 Immunocytochemical staining of α-SMA in normal control cells (a), shear stress control cells (b), and cells held under pressure of 50 cmH_2O for 2 h (c), 6 h (d), 12 h (e), and 24 h (f). Normal control cells presented scarce positive staining for α-SMA. In cells held under pressure of 50 cmH_2O, positive staining was prominent when the duration of the pressure was 12 h or 24 h. There was no obvious positive staining in the shear stress control group

epithelial morphology and cobblestone growth pattern, with scarce positive staining for α-SMA. In cells held under a pressure of 50 cmH_2O, positive staining was seen only when the duration of the pressure was 12 h or 24 h, and the staining was more prominent in the 24 h group than the 12 h group. There was no obvious positive staining in the shear stress control group.

Results from the Western blotting analysis are shown in Fig.5. By Western blotting analysis we detected that protein expression of α-SMA increased with increasing duration of pressure (Fig.6). Neither the normal control nor the shear stress control group displayed the expression of α-SMA protein. But among groups under the pressure of 50 cmH_2O for different duration, the 12 h and 24 h duration groups exhibited α-SMA protein expression and there was a statistical difference compared with the normal control and shear stress control groups (P<0.05). As shown in Fig.6, when the pressure of 50 cmH_2O was loaded to cells, the mRNA level of α-SMA in 12 h pressure-loading group was significantly higher than those of the normal control and shear stress groups (P<0.05) and it increased with increasing duration of pressure. This increase was more remarkable in 24 h pressure-loading group.

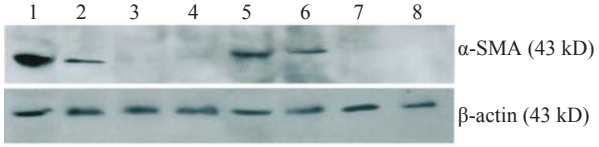

Fig.5 Western blotting analysis of α-SMA expression in NRK52E. Neither normal control nor shear stress control group displayed the expression of α-SMA protein. Cells held under pressure of 50 cmH_2O for 12 h, 24 h, 30 cmH_2O for 24 h, and 100 cmH_2O for 24 h exhibited remarkable α-SMA protein expression. Lane 1, 100 cmH_2O 24 h; 2, 30 cmH_2O 24 h; 3, shear stress control; 4, normal control; 5, 50 cmH_2O 24 h; 6, 50 cmH_2O 12 h; 7, 50 cmH_2O 6 h; 8, 50 cmH_2O 2 h

As shown in Fig.7 α-SMA protein expression increases with increasing pressure magnitude. All of the three 24 h pressure-loading groups showed statistical increases of α-SMA protein expression compared with the normal control and shear stress control groups (P<0.05). Compared with the shear stress control group α-SMA mRNA expression of 30 cmH_2O, 50 cmH_2O and 100 cmH_2O pressure-loading groups for 24 h statistically increased (P<0.05), with the increasing pressure magnitude (Fig.7).

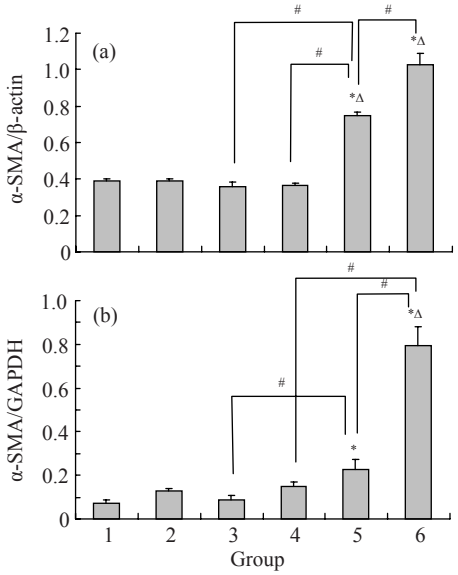

Fig.6 Protein and mRNA expression of α-SMA increased with increasing duration of pressure. Relative protein expression (α-SMA/β-actin) (a) and relative mRNA expression (α-SMA/GAPDH) (b) of α-SMA in normal control (group 1), shear stress control (group 2), cells held under pressure of 50 cmH_2O for 2 h (group 3), 6 h (group 4), 12 h (group 5) and 24 h (group 6). $^{*}P$<0.05 compared with the normal control group; $^{\Delta}P$<0.05 compared with the shear stress control group; $^{\#}P$<0.05 (n=6)

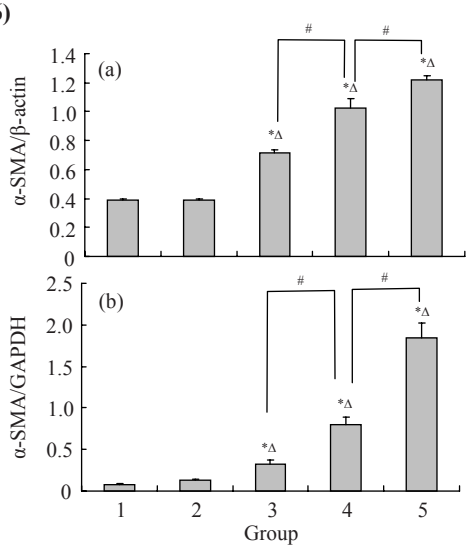

Fig.7 Protein and mRNA levels of α-SMA increased with increasing pressure magnitude. The three 24 h pressure-loading groups showed statistical increases of α-SMA protein and mRNA expression compared with the normal control and shear stress control groups. Relative protein expression (α-SMA/β-actin) (a) and relative mRNA expression (α-SMA/GAPDH) (b) of α-SMA in normal control (group 1), shear stress control (group 2), cells held under pressure of 30 cmH_2O for 24 h (group 3), 50 cmH_2O for 24 h (group 4), and 100 cmH_2O for 24 h (group 5). $^{*}P$<0.05 compared with the normal control group; $^{\Delta}P$<0.05 compared with the shear stress control group; $^{\#}P$<0.05 (n=6)

TGF-β1 expression changes of NRK52E cells under hydraulic pressure

As shown in Fig.8, the TGF-β1 mRNA expression of the normal control group was statistically different from that of 24 h pressure-loading groups (P<0.05), including the shear stress control group. However, compared with the shear stress control group, 30 cmH_2O and 50 cmH_2O pressure-loading for 24 h did not induce any change in TGF-β1 mRNA. Only the 100 cmH_2O pressure-loading for 24 h group showed a statistical increase in the expression of TGF-β1 mRNA compared with the shear stress control group (P<0.05). The changes in TGF-β1 mRNA expression in this study were induced by the combined action of hydraulic pressure and shear stress.

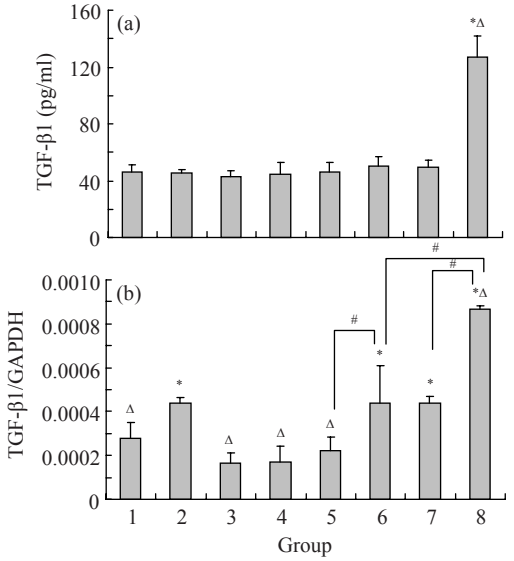

Fig.8 Changes in the expression of TGF-β1 of NRK52E under hydraulic pressure. The concentration of TGF-β1 in 100 cmH_2O pressure-loading for 24 h group was markedly higher than those of the normal control and shear stress control groups. There was no statistical difference among the rest groups. TGF-β1 mRNA expression of the normal control group was statistically different from those of 24 h pressure-loading groups, including the shear stress control group. Only the 100 cmH_2O pressure-loading for 24 h group showed a statistical increase in the expression of TGF-β1 mRNA compared with the shear stress control group. Concentration (a) and relative mRNA expression (b) of TGF-β1 in normal control (group 1), shear stress control (group 2), and cells held under pressure of 50 cmH_2O for 2 h (group 3), 6 h (group 4), 12 h (group 5), 24 h (group 6), 30 cmH_2O for 24 h (group 7), and 100 cmH_2O for 24 h (group 8). $^{*}P$<0.05 compared with the normal control group; $^{\Delta}P$<0.05 compared with the shear stress control group; $^{\#}P$<0.05 (n=6)

The concentration of TGF-β1 secreted from the NRK52E cells was measured by ELISA (Fig.8). Among the eight groups, only the concentration of TGF-β1 in 100 cmH_2O pressure-loading for 24 h group was markedly higher than those of the normal control and shear stress control groups (P<0.05). There was no significant difference among the rest groups.

DISCUSSION AND CONCLUSION

We examined whether hydraulic pressure can cause the TEMT that leads to renal fibrosis. To our knowledge, this is the first study to use a flow chamber apparatus to mimic the in vivo mechanical environment in experiments involving cultured NRK52E cells. Our study shows that hydraulic pressure can induce TEMT, which was observed as morphological changes, cytoskeletal changes, and de novo expression of the myofibroblast marker α-SMA. At the same time, TGF-β1 secretion increased in cells under pressure, which indicates that TGF-β1 may be involved in TEMT induced by hydraulic pressure.

First, our study showed that the cells exposed to hydraulic pressure of 50 cmH_2O for 24 h displayed a mildly spindle-like shape, elongation and loss of cell junctions, as well as microvilli on the cell surface under scanning electronic microscope. Our result was similar to that of previous studies, indicating that hydraulic pressure may induce TEMT, leading to a change in cell morphology from a cuboidal to a fibroblastic shape and the replacement of intracellular epithelial adhesion molecules by mesenchymal cytoskeletal markers (Zeisberg and Kalluri, 2004).

Second, our study showed that hydraulic pressure induces disorganization of F-actin filaments and the formation of curling clusters of F-actin in the cytoplasm, and that these effects increase when the pressure is applied for a longer duration. Cytoskeletal microstructure performs a crucial role in regulating cellular functions, which influence many biochemical processes. F-actin microfilaments are one of the primary protein filament components of the cytoskeleton (Palmer and Boyce, 2008). Given the crucial role of cytoskeletal microstructure in biological processes, the changes in the cytoskeleton observed in our study may be involved in TEMT. The results of our study are inconsistent with those of Martin *et al*.(2005),

whose work showed that under pressure of 60 cmH_2O microfilaments remained as elongated and continuous fibers extending along the entire length of the cell length for periods of applied pressure shorter than 3 d. Under 60 cmH_2O of pressure at 3 and 7 d, however, cells showed shorter microfilament fibers that were branched throughout the cell (Martin *et al*., 2005). The discrepancies between our study and that of Martin *et al*.(2005) may reflect the different cell types used or differences in the magnitude and type of mechanical forces exerted on the cells.

Third, and most important, finding in our study was that hydraulic pressure per se can induce the expression of the myofibroblast marker α-SMA in NRK52E cells, suggesting that hydraulic pressure can induce TEMT. Both gene expression and protein expression of α-SMA were significantly higher than those of the shear control group, when cells were subjected to pressures of 50 cmH_2O and 100 cmH_2O for 24 h. Furthermore, we demonstrated that α-SMA expression increased with increasing duration and magnitude of applied pressure. This result is similar to that of Sato *et al*.(2003), which showed that another kind of mechanical force (stretch) can induce TEMT in unilateral ureteral occlusion (UUO). Because the renal tubule was also affected by pressure in UUO, pressure may be involved in TEMT that occurs in UUO.

In the present study, we examined the expression of TGF-β1 in order to illustrate whether it participates in TEMT induced by hydraulic pressure. Our previous study identified TGF-β1 as an important profibrotic cytokine (Fan *et al*., 1999). Our present results are consistent with these findings. TGF-β1 mRNA expression was much higher in the group subjected to 100 cmH_2O pressure for 24 h than in the shear stress control group. Moreover, in the group subjected to 100 cmH_2O of pressure for 24 h, the TGF-β1 concentration in the supernatant was significantly higher than those of the rest groups. Some of these results are in accordance with several mechanical studies. Miyajima *et al*.(2000) have documented that mechanical stretch can induce an increase in TGF-β1 secretion and mRNA expression in NRK52E cells. Maruyama *et al*.(2005) found that hydrostatic pressure induced an increase in the concentration of TGF-β1 in supernatants of Madin-Darby canine kidney cells (Maruyama *et al*., 2005). In summary, the expression of TGF-β1 mRNA and protein was significantly up-regulated in the group subjected to 100 cmH_2O of pressure for 24 h, and this group also showed the maximum level of α-SMA, which indicates that TEMT induced by hydraulic pressure may involve TGF-β1. The TGF-β1 concentration in the supernatant statistically increased only in the group subjected to 100 cmH_2O of pressure for 24 h, but the increase of α-SMA protein increased with increasing magnitude and duration of applied pressure. This implies that the expression of α-SMA was not solely the result of TGF-β1.

In conclusion, we have shown for the first time that the mechanical force of hydraulic pressure induces TEMT in a magnitude- and duration-dependent manner, and that this pressure-induced TEMT is accompanied by TGF-β1 secretion. This process may involve changes in TGF-β1 expression. Our results suggest that increased hydraulic pressure in renal tubules may be one of the events underlying TEMT and renal fibrosis.

ACKNOWLEDGEMENTS

We appreciate the help from Dr. Xian-ming Mo and Wen-tong Meng of West China Hospital State Key Laboratory, Sichuan University. Our sincere thanks go to Hong Xie and Armando Chapin Rodriguez of West China Medical School, Sichuan University, for their help.

References

Cheng, M., Wu, J., Liu, X.H., Li, Y., Nie, Y.M., Li, L., Chen, H.Q., 2007. Low shear stress-induced interleukin-8 mRNA expression in endothelial cells is mechanotransduced by integrins and the cytoskeleton. *Endothelium*, **14**(6):265-273. [doi:10.1080/10623320701678169]

Cowger, N.L., Benes, E., Allen, P.L., Hammond, T.G., 2002. Expression of renal cell protein markers is dependent on initial mechanical culture conditions. *J. Appl. Physiol.*, **92**(2):691-700.

Deen, W.M., Maddox, D.A., Robertson, C.R., Brenner, B.M., 1974. Dynamics of glomerular ultrafiltration in the rat. VII: response to reduced renal mass. *Am. J. Physiol.*, **227**(3):556-562.

Essig, M., Friedlander, G., 2003. Shear-stress-responsive signal transduction mechanisms in renal proximal tubule cells. *Curr. Opin. Nephrol. Hypertens.*, **12**(1):31-34. [doi:10.1097/00041552-200301000-00006]

Essig, M., Terzi, F., Burtin, M., Friedlander, G., 2001. Mechanical strains induced by tubular flow affect the phenotype of proximal tubular cells. *Am. J. Physiol. Renal. Physiol.*, **281**(4):F751-F762.

Fan, J.M., Ng, Y.Y., Hill, P.A., Nikolic-Paterson, D.J., Mu, W., Atkins, R.C., Lan, H.Y., 1999. Transforming growth factor-beta regulates tubular epithelial-myofibroblast transdifferentiation in vitro. *Kidney Int.*, **56**(4):1455-1467. [doi:10.1046/j.1523-1755.1999.00656.x]

Gnudi, L., Thomas, S.M., Viberti, G., 2007. Mechanical forces in diabetic kidney disease: a trigger for impaired glucose metabolism. *J. Am. Soc. Nephrol.*, **18**(8):2226-2232. [doi:10.1681/ASN.2006121362]

Hostetter, T.H., Olson, J.L., Rennke, H.G., Venkatachalam, M.A., 1981. Hyperfiltration in remnant nephrons: a potentially adverse response to renal ablation. *Am. J. Physiol.*, **241**(1):F85-F93.

Kaufman, J.M., Siegel, N.J., Hayslett, J.P., 1975. Functional and hemodynamic adaptation to progressive renal ablation. *Circ. Res.*, **36**(2):286-293.

Klahr, S., Schreiner, G., Ichikawa, I., 1988. The progression of renal disease. *New Engl. J. Med.*, **318**:1657-1666.

Lehoux, S., Castier, Y., Tedgui, A., 2006. Molecular mechanisms of the vascular responses to haemodynamic forces. *J. Intern. Med.*, **259**(4):381-392. [doi:10.1111/j.1365-2796.2006.01624.x]

Martin, J.S., Brown, L.S., Haberstroh, K.M., 2005. Microfilament are involved in renal responses to sustained hydrostatic pressure. *J. Urol.*, **173**(4):1410-1417. [doi:10.1097/01.ju.0000149031.93643.a5]

Maruyama, T., Hayashi, Y., Nakane, A., Sasaki, S., Kohri, K., 2005. Intermittent pressure-loading increases transforming growth factor-beta-1 secretion from renal tubular epithelial cells in vitro vesicoureteral reflux model. *Urol. Int.*, **75**(2):150-158. [doi:10.1159/000087170]

Meguid El Nahas, A., Bello, A.K., 2005. Chronic kidney disease: the global challenge. *Lancet*, **365**(9456):331-340. [doi:10.1016/S0140-6736(05)17789-7]

Miyajima, A., Chen, J., Kirman, I., Poppas, D.P., Darracott Vaughan, E., Felsen, D., 2000. Interaction of nitric oxide and transforming growth factor-beta 1 induced by angiotensin II and mechanical stretch in rat renal tubular epithelial cells. *J. Urol.*, **164**(5):1729-1734. [doi:10.1016/S0022-5347(05)67097-8]

Mori, T., Cowley, A.W., 2004. Role of pressure in angiotensin II-induced renal injury chronic servo-control of renal perfusion pressure in rats. *Hypertension*, **43**(4):752-759. [doi:10.1161/01.HYP.0000120971.49659.6a]

Ohashi, T., Sugaya, Y., Sakamoto, N., Sato, M., 2007. Hydrostatic pressure influences morphology and expression of VE-cadherin of vascular endothelial cells. *J. Biomech.*, **40**(11):2399-2405. [doi:10.1016/j.jbiomech.2006.11.023]

Palmer, J.S., Boyce, M.C., 2008. Constitutive modeling of the stress-strain behavior of F-actin filament networks. *Acta Biomaterialia*, **4**(3):597-612. [doi:10.1016/j.actbio.2007.12.007]

Rodriguez-Pena, A., Prieto, M., Duwel, A., Rivas, J.V., Eleno, N., Perez-Barriocanal, F., Arevalo, M., Smith, J.D., Vary, C.P., Bernabeu, C., Lopez-Novoa, J.M., 2001. Up-regulation of endoglin, a TGF-β-binding protein, in rats with experimental renal fibrosis induced by renal mass reduction. *Nephrol. Dial. Transplant.*, **16** (Suppl. 1):34-39.

Sato, M., Muragaki, Y., Saika, S., Roberts, A.B., Ooshima, A., 2003. Targeted disruption of TGF-β1/Smad3 signaling protects against renal tubulointerstitial fibrosis induced by unilateral ureteral obstruction. *J. Clin. Invest.*, **112**(10):1486-1494. [doi:10.1172/JCI200319270]

Shin, H.Y., Gerritsen, M.E., Bizios, R., 2002. Regulation of endothelial cell proliferation and apoptosis by cyclic pressure. *Ann. Biomed. Eng.*, **30**(3):297-304. [doi:10.1114/1.1458595]

Silverman, M.D., Waters, C.R., Hayman, G.T., Wigboldus, J., Samet, M.M., Lelkes, P.I., 1999. Tissue factor activity is increased in human endothelial cells cultured under elevated static pressure. *Am. J. Physiol. Cell Physiol.*, **277**(2):233-242.

Suda, T., Osajima, A., Tamura, M., Kato, H., Iwamoto, M., Ota, T., Kanegae, K., Tanaka, H., Anai, H., Kabashima, N., Okazaki, M., Nakashima, Y., 2001. Pressure-induced expression of monocyte chemoattractant protein-1 through activation of MAP kinase. *Kidney Int.*, **60**(5):1705-1715. [doi:10.1046/j.1523-1755.2001.00012.x]

Wang, J.H.C., Thampatty, B.P., 2006. An introductory review of cell mechanobiology. *Biomech. Model. Mechanobiol.*, **5**(1):1-16. [doi:10.1007/s10237-005-0012-z]

Zavadil, J., Bottinger, E.P., 2005. TGF-beta and epithelial-to-mesenchymal transitions. *Oncogene*, **24**(37):5764-5774. [doi:10.1038/sj.onc.1208927]

Zeisberg, M., Kalluri, R., 2004. The role of epithelial-to-mesenchymal transition in renal fibrosis. *J. Mol. Med.*, **82**(3):175-181. [doi:10.1007/s00109-003-0517-9]